

Diagnostic set-up and modelling for investigation of synergy between 3D edge physics and plasma-wall interactions on Wendelstein 7-X

Y. Liang^{1,a}, O. Neubauer¹, R. König², M. Krychowiak², B. Schweer³, P. Denner¹, M. Rack¹, D. Reiter¹, Y. Feng², A. Krämer-Flecken¹, P. Drews¹, F. Hasenbeck¹, S. Liu^{1,4}, Y. Gao^{1,4}, E. H. Wang¹, Y. Wei¹, M. Dostal¹, L. Li^{1,5}, N. Wang^{1,6}, J. Geiger², Y. Suzuki⁷, S. Sereda¹, P. Börner¹, A. C. Weger¹, W. Biel¹, S. Brezinsek¹, A. Charl¹, G. Czymek¹, D. Höschen¹, F. Effenberg⁸, O. Grulke¹, D. Nicolai¹, H. T. Lambertz¹, O. Marchuk¹, O. Schmitz⁸, K. P. Hollfeld¹, M. Knaup¹, G. Offermanns¹, G. Satheeswaran¹, A. Terra¹, J. Thomas¹, T. S. Pederson², U. Samm¹, C. Linsmeier¹ and the W7-X team

¹ Forschungszentrum Jülich GmbH, Institut für Energie- und Klimaforschung-Plasmaphysik, Partner of the Trilateral Euregio Cluster (TEC), 52425 Jülich, Germany

² Max Planck Institute for Plasma Physics, 17491 Greifswald, Germany

³ Laboratoire de Physique des Plasmas-Laboratorium voor Plasmafysica, ERM/KMS, 1000 Brussels, Belgium

⁴ Institute of Plasma Physics, Chinese Academy of Sciences, Hefei 230031, China

⁵ College of Science, Donghua University, Shanghai 201620, China

⁶ State Key Laboratory of Advanced Electromagnetic Engineering and Technology, Huazhong University of Science and Technology, Wuhan, Hubei 430074, China

⁷ National Institute for Fusion Science, Japan

⁸ University of Wisconsin-Madison, Madison, WI, USA

^a Contact Email: [Y. Liang@fz-juelich.de](mailto:Y.Liang@fz-juelich.de)

Abstract: A set of edge diagnostics and modelling has been developed for investigation of synergy between 3D edge physics and plasma-wall interactions on Wendelstein 7-X. A set of endoscopes has been designed for visible and ultraviolet spectroscopy and tomography of the plasma edge, along with infrared thermography of the divertor tiles. Two-dimensional profiles of impurities (e.g. He, C) will be measured by two endoscopes viewing the island divertor region in the plasma edge with a spatial resolution of < 2 mm. A multipurpose manipulator, which is used as the carrier either of the probe head for measuring the plasma edge profiles or of samples for plasma exposure studies, was installed at the outside mid-plane on W7-X in 2015. A poloidal correlation reflectometer has also been installed at W7-X. The system consists of an antenna array observing the propagation of turbulent phenomena in the mid-plane. The EMC3-EIRENE code package has been adapted for plasma edge transport in helium plasma at Wendelstein 7-X using a hybrid fluid-kinetic approach by enabling EMC3 to treat non-hydrogen isotopes and extending the usage of EIRENE features within EMC3-EIRENE.

1. Introduction

Steady-state operation of future fusion power plants requires a solution for a tolerable plasma exhaust, including steady-state and transient heat and particle fluxes on plasma-facing components. Recently, applications of the three-dimensional (3D) magnetic topology for controlling the edge plasma transport, stability, and plasma-wall interactions (PWIs) have attracted much attention in fusion research, especially the use of resonant magnetic perturbation coils in tokamaks [1]. To investigate this physics issue, however, it is very likely that a superconducting stellarator device, which allows a long-pulse stable operation with an intrinsic 3D magnetic topology concept, will be of great benefit.

The superconducting stellarator Wendelstein 7-X (W7-X) [2], a drift-optimized stellarator with improved neoclassical confinement, is designed for an initially steady-state plasma operation with a maximum magnetic field strength on axis of 3 T, a major radius of $R_0 = 5.5$ m and an effective minor radius of $\langle a \rangle = 0.55$ m. One major objective of the W7-X experiment is to demonstrate steady-state divertor operation at high densities and high central

temperatures. Therefore, investigation of the role of 3D divertor concepts in the physics and control of edge transport and stabilities, heat and particle exhausts is essential.

In fact, plasma operation of W7-X follows a staged approach following the successive completion of the in-vessel components. Starting with a limiter configuration, the first W7-X experimental campaign OP1.1 has been successfully carried out. The second campaign OP1.2 has been scheduled for 2017. In this phase, plasma operation with a divertor configuration without water cooling will be implemented, and the total heat power will be upgraded from 5MW (ECRH only) to about 20 MW (ECRH: 8.8MW, NBI: 10MW (D)/ 7MW(H), ICRH: 1.6MW). The main goal of OP1.2 is the preparation of the steady-state phase.

2. Synergy between 3D edge physics and plasma-wall interactions on W7-X

The concept of W7-X for plasma exhaust uses the formation of an inherent separatrix at the boundary for creating a so-called island divertor. The confinement region is either limited by the separatrix of the boundary island chain or by an ergodized region formed by the remnants of overlapping high-order rational islands around the major resonance. Three major island divertor configurations with rotational transform values of $\iota=5/6$, $5/5$ and $5/4$ are available for use in the coming W7-X experimental campaign OP 1.2.

The PWI in the divertor region of W7-X will be of great importance for the operational phase OP1.2. While the erosion of the divertor will have an impact on its lifetime and is therefore a critical subject of investigation, fundamental PWI studies in the divertor region are in many ways equally significant. These PWIs will be influenced by impurity transport, where the complex 3D magnetic geometry will play a crucial role, but also the magnetic geometry itself will be influenced by plasma effects such as Pfirsch–Schlüter and bootstrap currents. In figure 1, the results calculated by the HINT2 code indicate that the width of the edge islands reduces gradually with an increase in plasma beta from 0% (vacuum assumption) to 3%. This will directly influence the distribution of the field line connection length and the performance of island divertor. Furthermore, the edge transport and stability, impurity screening effect, and

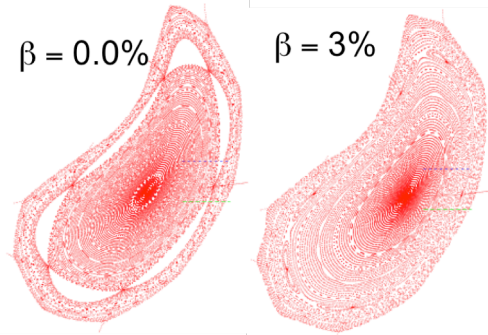


Figure 1 Beta dependence of the magnetic topology on W7-X. Here, the 3D equilibrium is calculated by the HINT2 code with a low- ι configuration. The magnetic islands are $n/m=5/6$.

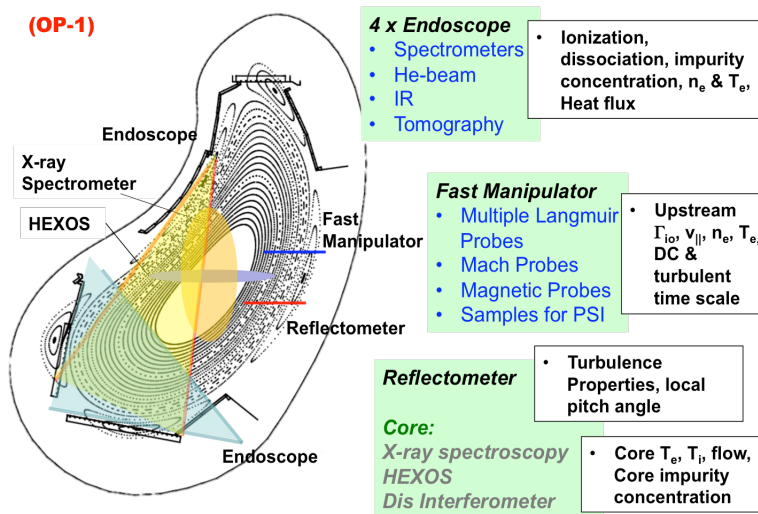


Figure 2 Diagnostics contributed from FZJ during the campaign OP 1.2 on W7-X

plasma-wall interactions will be affected self-consistently. Therefore, along with measurements of obvious quantities such as heat flux, PWI research in the divertor region will also require measurements of the temperature in the plasma edge and of the concentration and distribution of different impurities, in combination with modelling of impurity transport.

To investigate systematically the synergy

between 3D edge physics and PWI, a set of edge diagnostics [3] (see fig. 2) has been developed for the upcoming W7-X experiments and the EMC3-EIRENE code is being extended to helium plasmas for the OP1.1 phase.

3. Diagnostic set-up and modelling for 3D edge physics and plasma-wall interactions

3.1 Measurements of electron temperature, density, and impurity distributions in the divertor region, and heat flux on the local divertor target plate

In order to study the origin of impurities (C is expected to dominate in OP1.2) and edge impurity transport with different magnetic configurations of island divertor on W7-X, a set of endoscopes has been designed for visible and ultraviolet spectroscopy and for tomography of the plasma edge, along with infrared thermography of the divertor tiles [4]. Two-dimensional profiles of impurities (e.g. He, C) will be measured by two endoscopes viewing the island divertor region in the plasma edge with a spatial resolution of < 2 mm. The working spectral range of each endoscope is from 350 nm to 7000 nm. The light from the divertor plasma is divided equally into two branches by a prism in the detector box. Each branch is divided into ultraviolet (UV: 350 nm – 550 nm), visible (VIS: 550 nm – 950 nm) and infrared (IR: 950 nm – 7000 nm) sub-branches by dichroic filters. The ultraviolet and visible sub-branches are

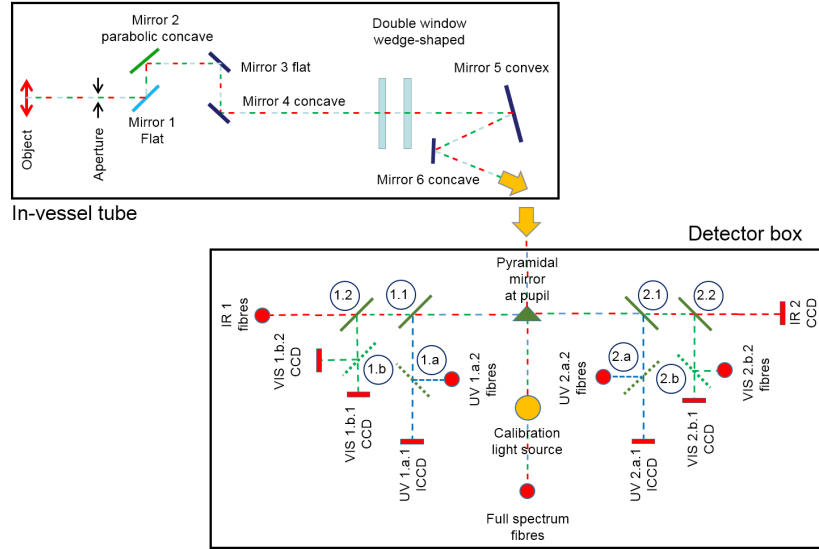


Figure 3 Optical layout of endoscope

divided again for the filter cameras and spectrometers as seen in Fig.3.

Each endoscope includes 5 filter cameras (2 UV and 3 VIS filter cameras), 1 infrared camera and 5 spectrometers (2 UV, 1 VIS, 1 IR and 1 overview spectrometer). The image size in the focal plane is 14 mm \times 14 mm, which is focused onto 14 fibers (diameter 1 mm) in an array by a cylindrical lens. The 14 fibers are connected to the spectrometer located in a laboratory. The spatial

resolution on the divertor plates is 2 cm - 3 cm. Two UV spectrometers use high- n Balmer spectroscopy to deduce electron density from Stark broadening, and electron temperature from line ratio or discrete-to-continuum transition. These two UV spectrometers could also be used to measure the CD Gerö and C2 Swan bands in order to study the chemical sputtering on the carbon divertor plates. The VIS spectrometer is used to measure the Fulcher band in order to study the hydrogen recycling on the divertor plates. The VIS spectrometer could also be used to measure helium lines in order to deduce electron density and temperature. The IR spectrometer is used to measure the Paschen series in order to deduce electron temperature and density.

An overview spectrometer, which can cover a wide wavelength range to monitor impurity contents in the divertor region, is linked to full-spectrum fibers located at the leading vertex of the pyramidal mirror in the endoscope system. The light from the plasma will be carried by several 1 mm diameter fibers to the diagnostics room, where it will be coupled to the five-channel overview spectrometer (Aventes model: AVASPEC-ULS2048L-USB2-RM). Each

channel is a miniature Czerny-Turner spectrometer with a fixed grating to cover a certain wavelength range. Together, these channels can cover the wavelength range from 300 to 1100 nm. This overview spectrometer will be used for routine investigation of the impurity contents under different operational scenarios. It will also provide reference data for other diagnostic equipment on the endoscope system, with which it shares the same field of view.

Through a pair of endoscopes, a high-resolution divertor infrared (D-IR) thermography system, which includes two medium-wavelength range (3-5 μm) infrared cameras, will be implemented on W7-X to monitor the temperature and to measure the heat flux on both the vertical and horizontal divertor targets in one toroidal cross section during in the campaign OP 1.2. This D-IR system has a high spatial resolution of less than 2 mm on the divertor target plate, and it will allow for a delicate study of the footprint patterns. With an optimized smaller field of view, measurements with high temporal resolution could be achieved to investigate transient events (i.e. Edge localized Modes) releasing large amounts of energy. The designed rotating mirror at the front-end of the endoscope enables poloidal scanning of the region of interest, thus the viewing area of the camera has the potential to be actively shifted during the operation for the strike line characterization under different configurations.

The whole endoscope system is currently under construction and will be installed on W7-X at the end of 2016. A similar system was successfully installed on JET (the world's largest tokamak) in 2012. In the W7-X experimental campaign OP1.2A, one 0.75m imaging Czerny-Turner spectrometer and two 0.75m Littrow spectrometers will be installed on the endoscope. In addition, a high-efficiency XUV overview spectrometer (HEXOS) has been used for monitoring impurity concentration in the plasma core.

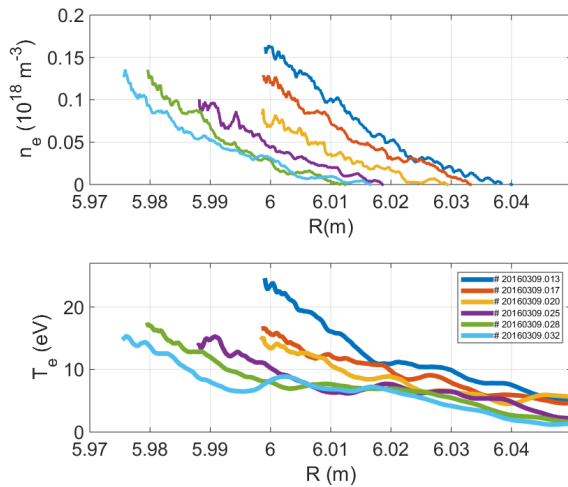


Figure 4 Edge profiles of electron density (n_e) and temperature (T_e) measured by the combined probe on W7-X with various inwardly shifted high-iota limiter configurations.

3.2 Measurement of edge upstream plasma profiles

A multi-purpose manipulator, which is used as the carrier either for measurements of the plasma edge profiles or for plasma exposure studies, was installed at the outside mid-plane on W7-X in 2015 [5, 6]. One of the most important features of the manipulator is the fast and stable movement of the probe. The maximum acceleration and velocity are 3 g and 3.5 m/s, respectively. A combined probe head, which measures the radial distribution of the magnetic field with magnetic pick-up coils, the plasma temperature and density profiles with Langmuir probes and the plasma flows with a Mach probe, was mounted on the manipulator and

commissioned during the campaign OP 1.1 [7]. For the next operational campaign, an improved design of the combined probe, a retarding field analyzer (RFA) and a dedicated Mach probe array will be employed. For plasma wall interaction studies, the ability to expose samples on the combined probe and on a dedicated heatable probe holder is planned.

The combined probe yielded good results for the edge profiles of the radial electric field, electron temperature and density and the magnetic field in the first campaign. The probe was able to measure both during a plunge and in a stationary position at the plasma edge. A series of scenarios with a tuning of the planar coils and a ramp of the iota was carried out. These

measurements showed that the combined probe is able to reliably measure the edge parameters (see fig. 4).

For plasma edge characterization and measurements of plasma parameters, particularly ion temperature, using an RFA is a well-known technique which has shown good results on various fusion devices. For W7-X, the combined RFA probe head contains two Langmuir pins to measure electron parameters and 2 back-to-back oriented RFA modules to measure the ion parameters simultaneously, each with 3 independent, radially shifted channels (see fig. 5). This combined RFA probe will be mounted on the fast multi-purpose manipulator on W7-X, so that it is possible to determine ion parameter profiles through the SOL up to several cm inside the separatrix. By adjusting the applied grid potentials, it is not only possible to determine ion parameters but also to use the probe head for multi-channel electron parameter measurements or high-energy particle loss measurements.

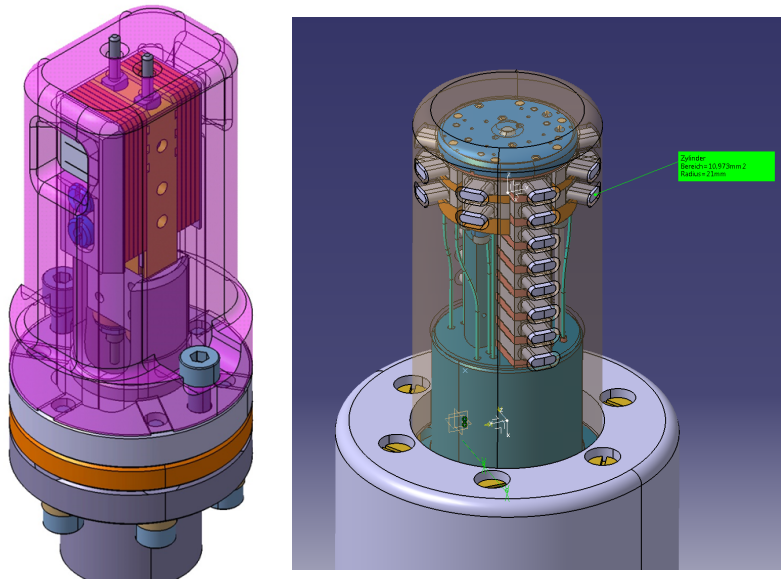


Figure 5 Sketches of the combined RFA probe (left) and the Mach probe (right) for W7-X

This probe head has a spatial resolution of 100 μm and a radial distance between the channels of 3 mm. To ensure that the probe head is always oriented along the magnetic field lines, independent of the chosen magnetic field configuration, it is possible to rotate the probe head manually before the experiment. Due to the high thermal loads, the slit plate for particle flux reduction inside the probe head and

for dividing the particle flux into the various channels and also the biased grids are made of tungsten. However, the cover is made of graphite. The design of the combined retarding field analyzer has been finalized. The first experiments are scheduled for the OP1.2 at W7-X.

To study the dynamics of edge flow profiles with different heating, gas fueling or impurity seeding in plasmas with different magnetic topology, a multi-array Mach probe, which includes 8 rows in the radial direction and 28 pins in total, is under construction for W7-X. Each of the top two rows includes 8 pins evenly distributed around the cylindrical probe, while other six rows include 2 back-to-back pins each, and they are oriented along the magnetic field lines. Each probe pin is made of tungsten and has a collecting area of 12 mm². Moreover the multi-array Mach probe measures edge profiles of particle fluxes with a high temporal resolution of few hundred kHz. Therefore, the characterization of edge transport for transient events is possible.

3.3 Measurements of edge turbulence and the pitch angle of field lines

Edge turbulence characteristics can be obtained by the Langmuir probes on the combined probe head, such as turbulence decorrelation time, cross correlation relationship and turbulence propagation along both the poloidal and radial directions, along with phase velocity, particle flux driven by turbulence and Reynolds stress. During the campaign OP1.1, the typical poloidal correlation length of turbulence was about 1 - 2.5 cm in the SOL region and decreased to ~ 1 cm inside the LCFS. Figure 6 shows a typical auto power spectrum from

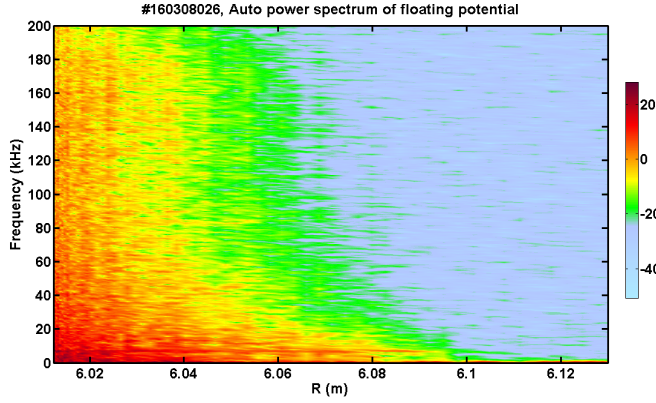


Figure 6 Auto power spectrum of the edge floating potential measured by Langmuir probes on W7-X in the limiter configuration.

the floating potential measured by Langmuir probes, with line averaged density $\langle n_e \rangle = 2.4 \times 10^{19} \text{ m}^{-3}$ and ECRH heating power $P = 4 \text{ MW}$ in the standard limiter configuration. A mode at frequency of $\sim 7 \text{ kHz}$ is observed as shown in figure 6. This mode can be detected at $R = 6.11 \text{ m}$, about 10 cm outside of the LCFS, and its amplitude increases significantly when close to the separatrix. It should be noted that the magnetic coils embedded in the combined probe head also measured this 7 kHz mode.

A poloidal correlation reflectometer has been installed at W7-X [8]. The system consists of an antenna array observing the propagation of turbulent phenomena in the midplane. The diagnostic operates in a bean shaped poloidal plasma cross section. The five antennae aim at the plasma edge ($R = 6 \text{ m}$, $Z = -0.104 \text{ m}$ and $\Phi = 71.05^\circ$). The system is operated in O-mode polarization, which limits the observation range to those reflection layers (r_c) which fulfill the condition $0.6 \times 10^{19} \text{ m}^{-3} < n_e(r_c) < 2 \times 10^{19} \text{ m}^{-3}$. Beside the spectral characterization of the turbulence, the system is capable of measuring the poloidal propagation of the turbulence from 6 different antenna combinations.

Moreover, the poloidal and toroidal separation of the system allows the inclination angle of the turbulence to be measured. Assuming that the turbulence is aligned to the magnetic field line, the pitch of the magnetic field line can be calculated. Deviation from the magnetic field line pitch can be considered to be caused by the limited toroidal correlation length of the investigated turbulence. Furthermore, measurements of the pitch will be attempted in the vicinity of the island divertor. The pitch is related to the iota in the island. Accessing this quantity enables the measurement of the topological parameter relevant for the flux diversion: the field line connection length. In the island divertor of W7-X, this length is calculated from the internal rotational transform inside the island.

Another relevant topic is the existence of zonal flows. These flows are characterized in that a temporal increase in the flow velocity can be determined by the instrument. To be able to measure transient events with sufficient time for averaging the temporal resolution of the diagnostic is 4MHz. This should allow the measurement of velocities in less than 1ms. The system has been in operation since December 2015, and data are taken on a daily basis. In addition, the reflected signal is used as indication of the achieved plasma density, because the reflection condition depends on the local plasma density.

3.4 Modeling for 3D Edge transport and heat load distributions

Understanding the plasma exhaust processes in stellarators requires 3D transport models that are capable of dealing with transport processes in a stochastic field where closed flux surfaces do not exist. For this, the 3D plasma edge Monte Carlo code EMC3 will be used in connection with the W7-X island divertor experiments.

The fluid edge plasma Monte-Carlo code in three dimensions (EMC3) [9] coupled to the kinetic (neutral) transport code EIRENE [10, 11] is a commonly used plasma edge simulation code for treating complex magnetic configurations. EMC3-EIRENE has been continuously

improved and verified, but one remaining restriction up to now had been that the bulk ion species was limited to hydrogen isotopes, with higher-Z ions being treated as trace-impurities.

However, in initial operational phases, W7-X was operated with helium plasma. Computational quantification of helium plasma flows in the edge is required to extend the understanding of the involved physical processes. Therefore, an approach was studied to simulate helium plasma by slightly extending EMC3 to facilitate a treatment of the main plasma species with $Z \neq 1$ and expanding the use of EIRENE features within EMC3.

A zero dimensional estimate of the ionization and population distributions using collisional-radiative rate coefficients by McWhirter and Hearn [12] and Fujimoto [13] as well as estimated transport losses (via HYDKIN [14]) indicates that a reasonable treatment of helium plasma as a single-fluid system with helium in the second ionisation state is justified for limiter plasmas at W7-X ($n_e > 1 \times 10^{13} \text{ cm}^{-3}$ and $T_e > 20 \text{ eV}$).

A second estimate for the correct treatment of helium plasma can be made based on EIRENE test simulations by comparing the recycling flux from the targets with fluxes from volume-recombination. The simulations show that the dominant source for He^+ ions under the given conditions is ionization from helium atoms rather than volume-recombination from He^{++} ions. Thus, it leads to the same conclusion as the zero-dimensional estimate: helium in the second ionization state is dominant in the bulk of the plasma edge. Furthermore, this can be strengthened by comparing the simulated spatial distribution of neutral helium, He^+ , and He^{++} in a typical limiter discharge at W7-X (see fig. 7). Here, shown for a poloidal cross-section similar to that seen by the multi-purpose manipulator.

A treatment of neutral helium and He^+ ions is also required for a sufficient consideration of plasma wall interactions, which can be performed using the kinetic transport code EIRENE. In the simplest approach, the He^+ ions can be considered to have a distribution function that is a general solution of the Boltzmann equation. Therefore, an adequate treatment of He^+ ions is drift kinetic, incorporating transport effects at least at a certain level. The simplest transport model employed consists of following the He^+ ions in the test particle picture. Trajectory integration is carried out in the guiding center approximation, ignoring drift motion or anomalous transport. Processes like $\text{He}-\text{He}^+$ charge-exchange are considered via

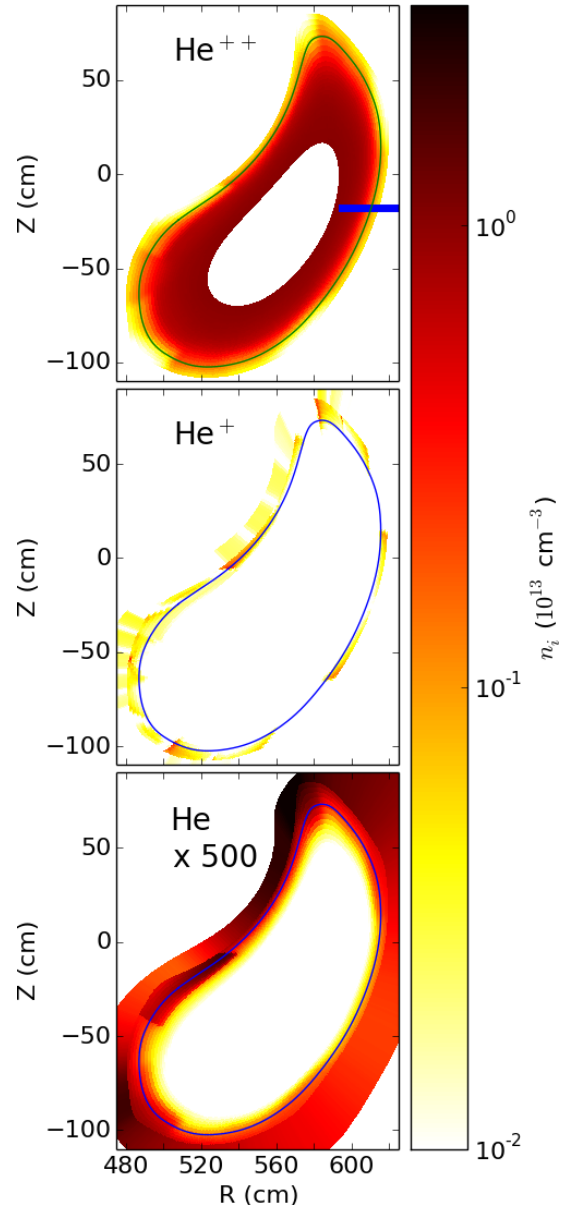


Figure 7 Comparison of neutral helium, He^+ , and He^{++} density distributions calculated for a typical W7-X limiter plasma with an averaged upstream ion density of $\langle n_i \rangle_{\text{LCFS}} = 0.5 \times 10^{13} \text{ cm}^{-3}$ and a heating power of $P = 2 \text{ MW}$. The blue line indicates the location of the multi-purpose manipulator and the solid line represents the LCFS.

the non-linear collision model of EIRENE. The dominant ion species He^{++} is treated with the fluid approach using a generalized model for EMC3 allowing for non-hydrogen isotopes.

4. Summary

Synergy between edge and divertor physics and plasma–wall interaction (PWI) will be of great importance for the operational phase OP1.2, in which various island divertor configurations will be applied for the first time on W7-X. These plasma–wall interactions will be influenced by impurity transport, where the complex 3D magnetic geometry will play a crucial role, but this magnetic geometry could itself be influenced by plasma effects. Therefore, in order to investigate systematically the synergy between 3D edge physics and the PWI, a set of edge diagnostics and modeling has been developed in combination with modeling of impurity transport on W7-X.

Acknowledgments

This work has been carried out within the framework of the EUROfusion Consortium and has received funding from the Euratom research and training programme 2014-2018 under grant agreement No 633053. The views and opinions expressed herein do not necessarily reflect those of the European Commission.

The authors gratefully acknowledge the computing time granted on the supercomputer JURECA [15] at Jülich Supercomputing Centre (JSC).

References:

- [1] Liang, Y., *et al.*, “Mitigation of type-I ELMs with $n=1, 2$ fields on JET with ITER-like wall”, Nucl. Fusion 53 (2013) 073036;
- [2] Wolf, R. C. *et al.*, “Wendelstein 7-X Program—Demonstration of a Stellarator Option for Fusion Energy”, IEEE TRANSACTIONS ON PLASMA SCIENCE, (2016)
- [3] Neubauer, O., *et al.*, “Diagnostic setup for investigation of plasma wall interactions at Wendelstein 7-X”, Fusion Engineering and Design, 96–97 (2015) 891–894
- [4] Neubauer, O., *et al.*, “Optical Instruments for Local Divertor Observation at Wendelstein 7-X.” 1st EPS Conference on Plasma Diagnostics (ECPD). 2015.
- [5] Nicolai, D., *et al.*, “A Multi-Purpose Manipulator system for W7-X as user facility for plasma edge investigation”, submitted to 29th SOFT (2016)
- [6] Satheeswaram, G., *et al.*, “A PCS7-based control and safety system for operation of the W7-X multi-purpose manipulator facility”, submitted SOFT (2016)
- [7] Drews, P., *et al.*, “Measurement of the plasma edge profiles using the combined probe on W7-X”, in this conference.
- [8] Krämer-Flecken, A., *et al.*, “Investigation of turbulence rotation in limiter plasmas at W7-X with a new installed Poloidal Correlation Reflectometry”, in this conference.
- [9] Feng, Y., *et al.*, “3D fluid modelling of the edge plasma by means of a Monte Carlo technique”, Journal of Nuclear Materials, 266-269, 812 (1999).
- [10] EIRENE. <http://www.eirene.de>.
- [11] Reiter, D., *et al.*, “The EIRENE and B2-EIRENE Codes”, Fusion Science and Technology, 47 (2), 172 (2005).
- [12] McWhirter, R.W.P., *et al.*, “Calculation of the Instantaneous Population Densities of the Excited Levels of Hydrogen-like Ions in a Plasma”, Proceedings of the Physical Society, 82 (5), 641 (1963).
- [13] Fujimoto, T., “A collisional-radiative model for helium and its application to a discharge plasma”, Journal of Quantitative Spectroscopy and Radiative Transfer, 21 (5), 439 (1979).
- [14] HYDKIN. <http://www.hydkin.de/>.
- [15] Jülich Supercomputing Centre. (2016). JURECA: General-purpose supercomputer at Jülich Supercomputing Centre. Journal of large-scale research facilities, 2, A62. <http://dx.doi.org/10.17815/jlsrf-2-121>